



# Work Function of Metal Back Contact Surface Alloy Molybdenum (Mo) With Tungsten (W) For Copper Indium Gallium Selenide (Cigs) Thin Film Solar Cell: Simulation Using Scaps-1d And Density Functional Theory (Dft) Using Winmostar Quantum Espresso

Imran Hindustan<sup>1\*</sup>, Niza Mohd Idris<sup>1</sup>, Mohd Khanapiah Nor<sup>1</sup>, Farah Shahnaz Feroz<sup>1</sup>, Zaiful Annuar Zainal<sup>2</sup>

<sup>1</sup>Faculty Technology dan Kejuruteraan Elektronik dan Computer (FTKEK), university Technical Malaysia Melaka, Melaka, Malaysia (UTeM)

<sup>2</sup>R&D Department, Perodua Manufacturing Sdn Bhd, Malaysia

\*Corresponding author

DOI: https://dx.doi.org/10.47772/IJRISS.2025.910000007

Received: 30 September 2025; Accepted: 06 October 2025; Published: 01 November 2025

# **ABSTRACT**

The rapid growth in today's electronic technology and usage leads to a high demand of electrical power consumptions. Researchers around the globe are continuing finding for renewable sources of energy to meet the increasing demands of energy. This is because the high fossil fuel and carbon consumptions contribute greatly on the emissions of carbon dioxide (CO<sub>2</sub>) and other greenhouse gases which have become the primary contributor of global climate change. Global temperatures have risen sharply over the last few decades and the atmospheric concentrations of CO<sub>2</sub> continue to rise while the global emissions have not yet peaked [1]. Research and development of CIGS solar cells was started in 1980s as one of the various renewable sources of energy. CIGS thin film solar cells efficiency remains become an interesting topic among the researchers. University of Maine achieved 5.8% CIGS thin film solar cells efficiency in 1976. The efficiency has significantly improved since then to 23.6% in 2023 by Evolar/UU [3]. This study aims to improve the efficiency by focusing on the metal back contact of the CIGS thin film solar cells. The simulations were conducted using SCAPS-1D and Winmostar Quantum Espresso for quantum chemical, molecular dynamics and first-principles calculations simulation tools. Back contact layer of CIGS solar cell acts as an optical reflector to reflect light back to the absorber layer. Molybdenum (Mo) is commonly used as the back contact because it forms low resistivity ohmic contact to CIGS absorber layer and has high conductivity. Furthermore, its conductivity does not degrade during deposition of CIGS at high substrate temperature, and it does not react strongly, chemically, with CIGS absorber layer. However, work function property of Mo is within the range of 4.36 eV to 4.95 eV. There is a need to increase the work function property of the back contact to improve carrier collection near the back contact. The findings from the study offers a critical insight into factors that could further improve the CIGS solar cells efficiency.

**Keywords:** Renewable energy; CIGS thin film solar cells; SCAPS-1D; Winmostar Quantum Espresso; Metal work function

# INTRODUCTION

Global temperatures and greenhouse gas concentrations especially CO<sub>2</sub> have risen sharply from 1990 onwards as compared than 1961 until 1990 baseline [1]. This in turns causes of global climate change which affects ecological, physical and health impacts including extreme weather events such as droughts, storms, heatwaves, floods, altered crop growth as well as disrupted water systems. Countries such as the US, UK, Malaysia and many others have implemented climate and energy policies to at least slow down growth in CO<sub>2</sub> and other greenhouse gas emissions. Among key actions to reduce greenhouse gas emissions is by transitioning to low

ISSN No. 2454-6186 | DOI: 10.47772/IJRISS | Volume IX Issue X October 2025



carbon alternatives for energy resources such as renewable energies. Under the 12<sup>th</sup> Malaysia Plan, Malaysia moves to implement low carbon, clean and resilient development up to 45% reduction in greenhouse gas emissions from 2005 measurements by 2030. Renewable energy resources include solar energy, wind, geothermal, biomass, hydroelectric and tidal energy. Photovoltaic systems convert direct sunlight into electricity through the use of solar cells. The 1<sup>st</sup> generation of solar cells includes monocrystalline and polycrystalline silicon, while the 2<sup>nd</sup> generation (thin-film PV) includes hydrogenated amorphous silicon (a-Si:H), Cadmium Telluride (CdTe), Copper Indium Gallium diSelenide (CIGS) and Copper Zinc Tin Sulfide (CZTS). The 3<sup>rd</sup> generation includes Dye-sensitized solar cells (DSSC), organic, perovskite and quantum dot.

This paper is structured as follows: The next section provides a detailed literature review on existing studies about CIGS thin-film solar cells, and the current CIGS thin-film solar cells performance. The methodology section outlines the research design including the simulations using SCAPS-1D and density functional theory using Winmostar Quantum Espresso software. The results section presents the findings from the simulations, highlighting the factors that contributes the solar cells performance. Finally, the discussion and conclusion section discuss the implications of these findings to improve the CIGS thin-film solar cells performance.

# RESEARCH BACKGROUND AND MOTIVATION

CIGS thin-film solar cells first fabricated at Bell Laboratory in 1974 with 5% efficiency. Currently a high conversion efficiency achieved at 23.6% by Evolar/UU in 2023 [3]. CIGS solar cells consist of TCO and buffer layer with n-type semiconducting material, absorber layer with p-type, and can be deposited on substrates such as glass, metal foils and polymers. Metal foils and polymers allow for applications that require lighter-weight or flexible modules.

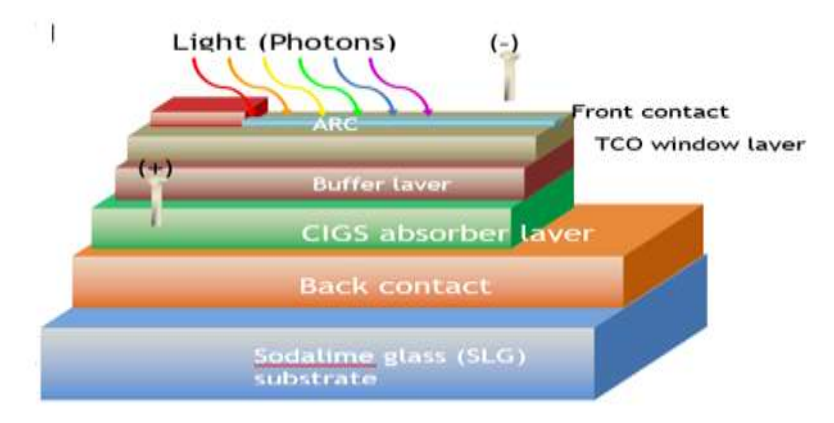


Figure 1: CIGS solar cell structure

Figure 1 shows the respective layers in a CIGS thin-film solar cells. The front contact consists of Aluminium (Al) grid. This layer helps to improve current collection of the solar cells. However, the metallic grid can cause an additional optical shading, reducing even more of the optical performance. Anti-reflection coating (ARC) may be constructed of MgF<sub>2</sub> ARC. The usage of ARC is crucial due to the fact that a large part of the optical loss happens at the front contact caused by reflections. The next layer is the Transparent Conductive Oxide (TCO) window layer. The TCO window layer may consists of materials such as ZnO, ITO, or Sano. TCO layer should has sufficient transparency to let enough light through to buffer layer underneath it. It should also have sufficient conductivity to transport the photogenerated current to the external circuit without too much resistance losses. Meanwhile, a buffer layer may consists of materials such as CdS or ZnS. For conventional heterojunction solar cells, n-type semiconductor CdS is used as a buffer layer because of its tunable bandgap 2.4 eV and good transparency. It also allows high incident photons to pass through and form a p-n junction with CIGS absorber layer. However, the CdS is a toxic and rare element that bounds their large-scale sustainable production. This is followed by CIGS absorber layer which is a p-type semiconducting material. CIGS is a chalcopyrite compound semiconductor alloy of group I-III-VI with high absorptivity (absorption coefficient of about 10 m). Its energy bandgap is in the range of 1.06 eV to 1.7 eV. Researchers gain interests in CIGS for thin-film solar cells because it has high conversion efficiency, high stability, and tunable bandgap. The back contact layer is consisted of Molybdenum (Mo). The back contact layer functions as an optical reflector to reflect the light back to the absorber layer. Mo is usually used as the back contact because it does not react strongly with CIGS absorber

ISSN No. 2454-6186 | DOI: 10.47772/IJRISS | Volume IX Issue X October 2025



layer. It also forms low resistivity ohmic contact to CIGS, and has high conductivity and does not degrade during deposition of CIGS absorber layer at high substrate temperature. Other than that, Mo is more chemically and mechanically stable during CIGS growth (during selenization process) as compared to other materisls. During selenization process, Se vapor will react with Mo to form an interfacial MoSe<sub>2</sub> layer. This interfacial layer has a wider bandgap (1.35eV to 1.41eV) than CIGS, enabling it to absorb more near infrared light to improve the cell performance. All these layers are deposited on substrate such as sodalime glass, or other flexible substrates such as metals and polymers. Sodalime glass (SLG) substrate is widely used in CIGS thin-film solar cells due to fact that it can supply sufficient amount of sodium (Na) to the absorber during co-evaporation or selenization processes. The supply of Na at 0.1 at% is reported to be beneficial for CIGS solar cells in terms of increasing the  $V_{\rm OC}$  and FF that lead to an enhancement in the cell efficiency. Na helps to passivates the defects at CdS and CIGS p-n junction. Other reasons SLG is chosen as the substrate are because it has a good adhesion, low weight, able to work on suitable temperature, optimal coefficient of thermal expansion for CIGS (5 × 10<sup>-6</sup> to  $12 \times 10^{-6}$  K<sup>-1</sup>) to avoid adhesion problem or crack formation during deposition of CIGS absorber layer at high temperature.

# The Need to improve the CIGS thin-film solar cells efficiencies.

Over the years, group of researchers are working hard to improve the efficiencies of thin-film solar cells including CIGS. Efficiency of a solar cell is a ratio of the solar cell output to input energy from the sun rays. Improving the solar cell efficiency resulted to not only making the solar cell technology a cost-competitive as compared the existing conventional sources of energy, but also ensures the maximum sun ray conversion and utilization of the installed hardware system.

The first CIGS solar cells were first fabricated at Bell Laboratory in 1974 with 5% efficiency. The current CIGS solar cells efficiency as recorded in [3] is 23.6% in 2023 by Evolar/UU. It shows a promising improvement in this field.

Back contact layer of CIGS thin-film solar cells acts as an optical reflector to reflect light back to the CIGS absorber layer. Despite the advantages of using Mo as the back contact, however, its work function property is within the range of 4.36eV to 4.95eV. There is a need to increase the work function property of the back contact, to improve carrier collection near the back contact.

# LITERATURE REVIEW

In 2023, Evolar/UU achieved power conversion efficiency of 23.6%. Solar Frontier achieved 22.3% efficiency in 2015 on a 0.5 cm² sized CIGSe solar cell by exploiting benefits of K treatment of the absorber surface. Kato et. al. improved the efficiency to 22.9% in Atsugi Research Center by using heavier alkali Cs treatment, which resulted from enhancements of both in V<sub>OC</sub> and in FF via the absorber modification. Alkali metal Cs treatment was chosen to improve carrier lifetime. The Cs-treated absorbers were subject to a CBD of CdS to make the buffer layer, followed by metal-organic CVD of ZnO:B to serve as TCO layer, and then MgF<sub>2</sub> deposited by evaporation to function as ARC.

Gunawan et. al. found that the activation energy of CZTSSe is significantly lower than its corresponding bandgap, which is usually ascribed to recombination at the interface. The recombination process at the back interface between the absorber and the back contact is serious because of the unfavorable energy band structure between CZTSSe and Mo. Mo with a lower work function compared to CZTSSe create a mismatch that arouses Schottky contact with a back contact barrier between absorber layer and metal back contact. MoSe2 interfacial layer existing between absorber and Mo film can convert the Schottky contact to a quasi-ohmic contact.

[5] tailored the work function of the back contact with Phosphorus (P) anion without any other layer introduced between Mo and absorber layer to adjust the carriers' collection in the back contact region. They found that the work function of the Mo back contact, processed with  $Na_3PO_4$  solution, was raised from 4.68eV to 5.62eV, thus a more desirable band alignment was obtained and the  $V_{OC}$  increased. They concluded that P diffused into Mo film and bound to Mo as P anion. The high work function back contact reduces the potential barrier at the back interface and introduces an electric field to suppress the recombination of photogenerated electrons and holes.



The electron work function of Mo and Tungsten (W) are the highest when they are at (110) plane [6]. The reflectivity curves of Mo and W are so nearly alike. Both Mo and W are widely used for their characteristics such as corrosion resistance, excellent conductivity and extremely high melting point [7]. Table 1 shows the characteristics comparison between Mo and W.

	Мо	W
Periodic table	Metal in Group VI B	Metal in group VI B
Atomic No	42	74
Atomic weight	95.94	183.85
density	10.2 g/cm <sup>3</sup>	19.3 g/cm <sup>3</sup>
Melting temperature	2610 °C	3410 °C
Atomic radius	0.139 nm	0.141 nm
Crystal structure	BCC at room temperature	BCC in the solid state
Lattice parameter	a = 0.315 nm	a = 0.316  nm

Table 1: Characteristics Comparisons between Molybdenum (Mo) and Tungsten (W)

# **METHODOLOGY**

This study begins with simulations of CIGS solar cell using Solar Cell Capacitance Simulator (SCAPS-1D). SCAPS-1D is a one-dimensional solar cell simulation program developed at the Department of Electronics and Information systems (ELIS), University of Gent, Belgium. It was originally developed for cell structures of CuInSe2 and CdTe. Recent developments applicable to crystalline solar cells (Si and GaAs) and amorphous cells (a-Si and micromorphous Si). Figure 2 shows the user interface of SCAPS-1D.

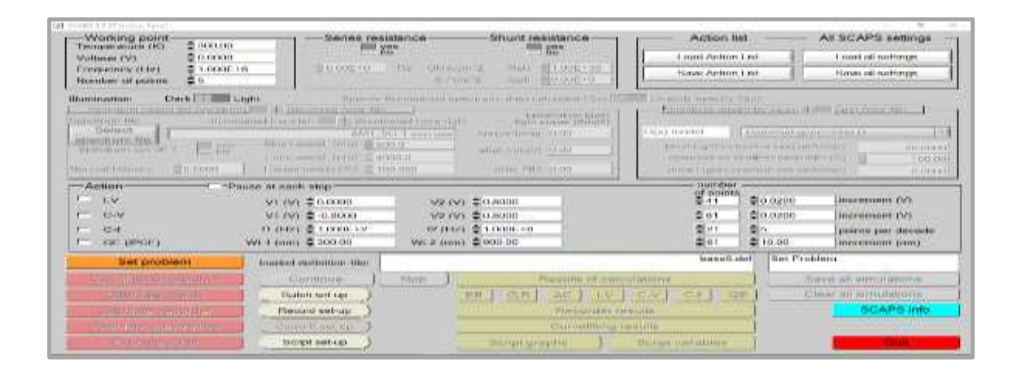




Figure 2: SCAPS-1D user interface.



The CIGS solar cell is then simulated with input parameters as shown in Table 2 and the cell structure is as shown in Figure 3 below.

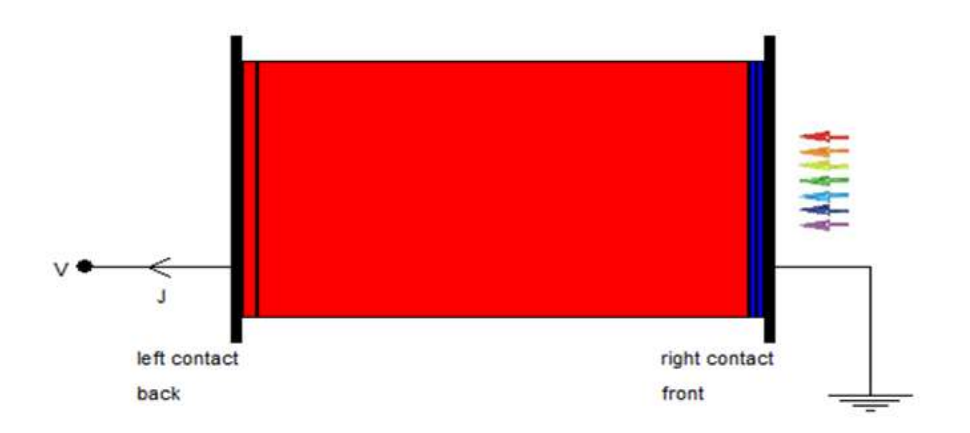


Figure 3: CIGS solar cell device structure

The output results of the simulation such as open circuit voltage Voc, short circuit current Jsc, Fill Factor (FF), and solar cell efficiency at various MoW metal work function values are as shown in Figure 6, 7, 8 and 9 respectively. The J-V curve and EQE of the CIGS solar cell at various MoW work function values is shown in Figure 10 and 11 respectively. Finally, the band diagram of the CIGS solar cell is as shown in Figure 12.

After the CIGS solar cell simulation using SCAPS-1D, the study continues with numerical simulation of metal work function for molybdenum Mo, tungsten W, and Mo alloyed with W, utilizing density functional theory (DFT) using Winmostar Quantum Espresso software. The software is very useful for quantum chemical, molecular dynamics and first-principles calculations. Figure 4 shows the user interface of Winmostar Quantum Espresso software.

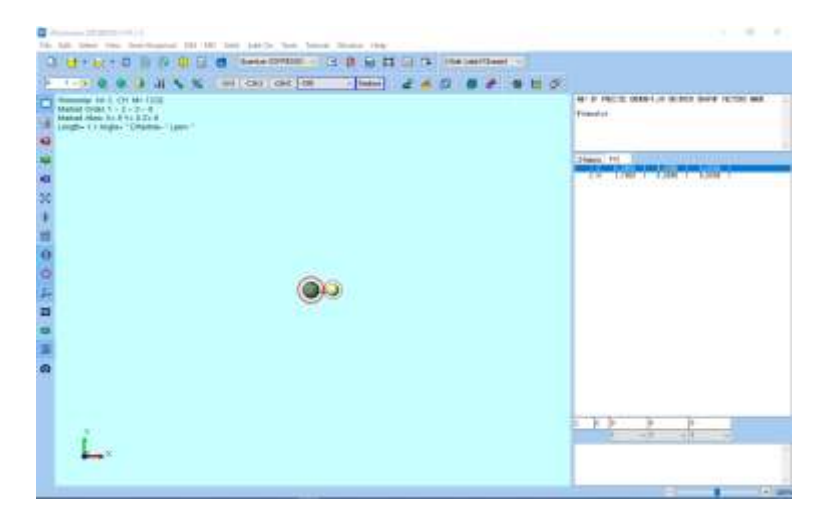


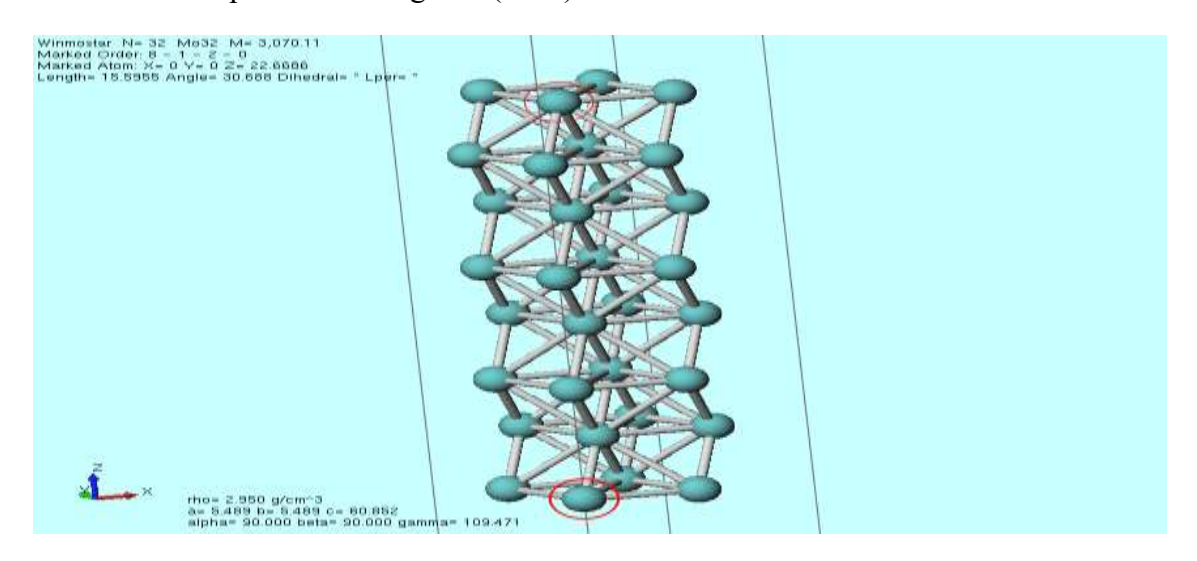
Figure 4: Winmostar Quantum Espresso software.

For the start, metal work functions at certain cutoff energy and K-points for several metals namely Ag, aluminium Al, aurum Au, molybdenum Mo and tungsten W are calculated and the results are tabulated in Table 3. The results then compared with [6] to check whether the simulation calculations gathered are valid. The results then tabulated as shown in Table 4.

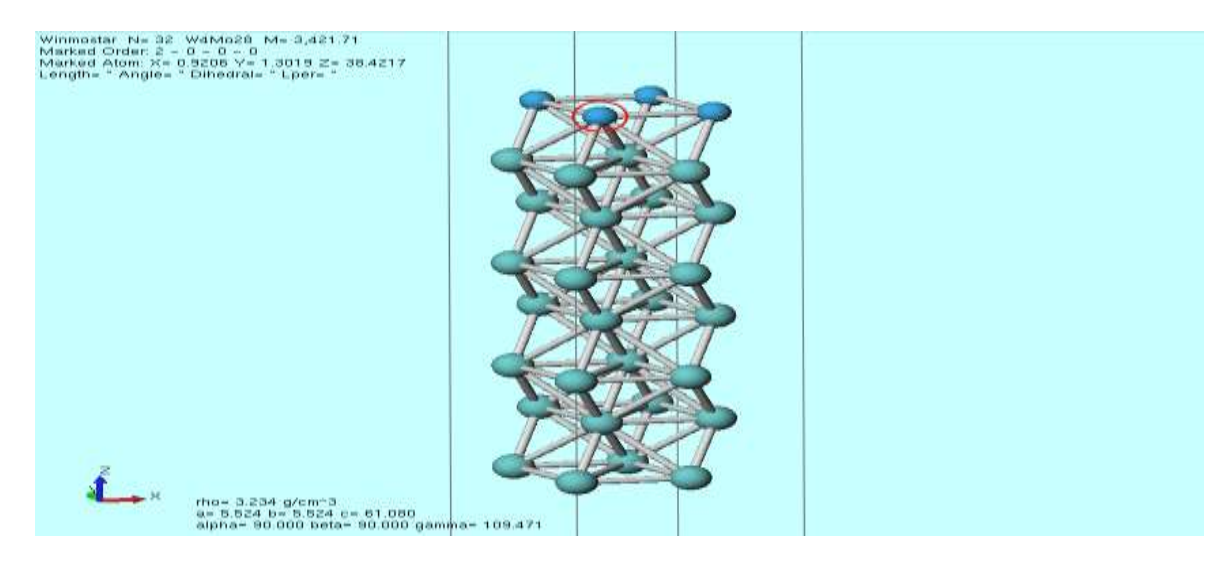
The next step is to calculate the Mo work function at plane (111), (110), (100) and (310). The results then compared with [6] and [10] to validate the calculation simulations. The results are tabulated as shown in Table 5.



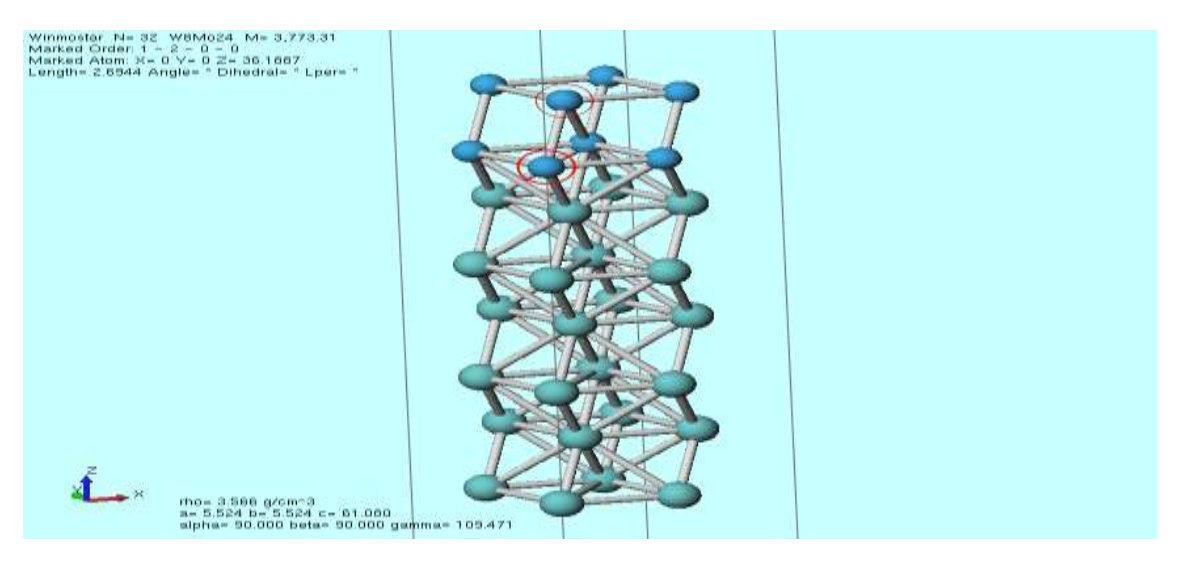
After that, calculation simulations of Mo alloyed with W are carried out by replacing the Mo atoms on the metal surface with tungsten W atoms at various Mo and W atom percentage, layer by layer, at (110) plane because the result shows Mo work function value is the highest at (110) plane. The steps of replacing the Mo atoms with W atoms are as depicted as in Figure 5(a-d).



(a)

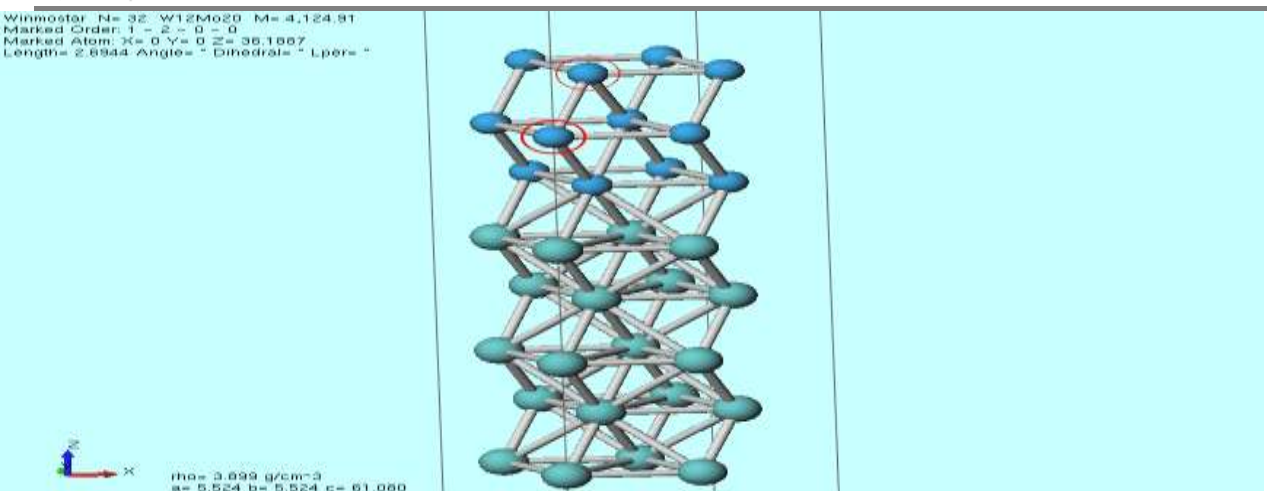


**(b)** 



(c)





(d)

Figure 5 (a-d): Steps of replacing Mo atoms with W atoms

The calculation simulations of the MoW metal surface work function are tabulated in Table 7. Table 6 shows the comparison between the calculated work function values with [6] and [10].

# FINDINGS AND DISCUSSIONS

4.1 Simulations using SCAPS-1D software

Table 2: CIGS solar cell input parameters using SCAPS-1D

Parameters	ZnQ.	CdS	CIGS	MoSe <sub>2</sub> [10]
Thickness (um)	0.05	0.05	3	0.1
Bandgap (eV)	3.3	2.4	1.2 1.12	1.1
Electron Affinity (eV)	4	3.8	4.1	4.14
Relative permittivity	9	10	13.6	8.6
Effective DOS, Nc_(cm-3)	2.22E+18	2.22E+18	2.22E+18	5.66E+17
Effective DOS, Nv (cm-3)	1.78E+19	1.78E+19	1.78E+19	2.41E+18
Electron thermal velocity (cm/s)	1.00E+07	1.00E+07	1.00E+07	4.13E+07
Hole thermal velocity (cm/s)	1.00E+07	1.00E+07	1.00E+07	2.55E+07
Electron mobility (cm2/V-sec)	1.00E+02	1.00E+02	1.00E+02	40.00
Hole mobility (cm2/V-sec)	2.50E+01	2.50E+01	2.50E+01	10.00
Donor concentration, ND (cm-3)	1.00E+18	1.00E+17	0	10.00
Acceptor concentration, NA (cm-3)	0	0	9.80E+16	1.00E+16
Bulk defect type	single d	single d	single a	d
Bulk defect concentration (cm-3)	1.00E+17	1.00E+18	1.00E+14	no defect (ideal)

Table 2 shows all the parameters being used in simulations using SCAPS-1D for each layer including buffer, Cu(InGa)Se absorber layer and MoSe<sub>2</sub> layers. These parameters are fixed for the purpose of this study, and the only changing parameter is the work function value of the back contact. This is important to investigate how the CIGS solar cell performance is effected by the back contact work function values.

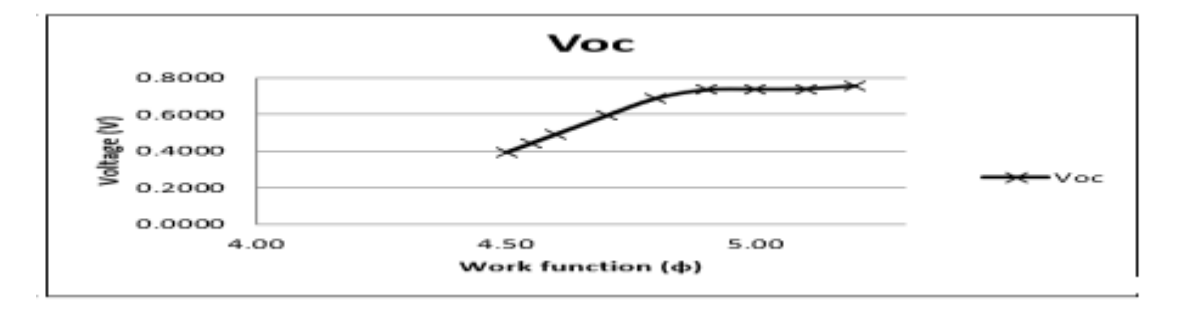


Figure 6: Voc at various MoW metal work function



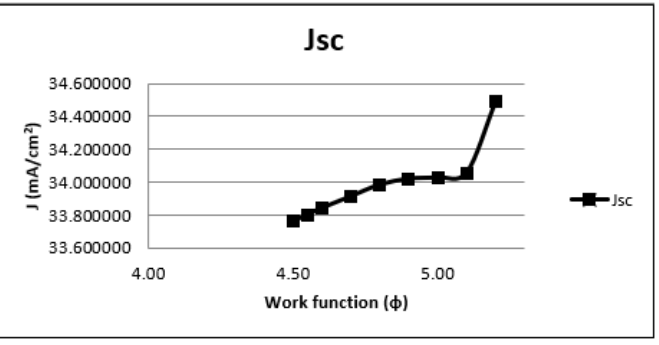


Figure 7: Jsc at various MoW metal work function

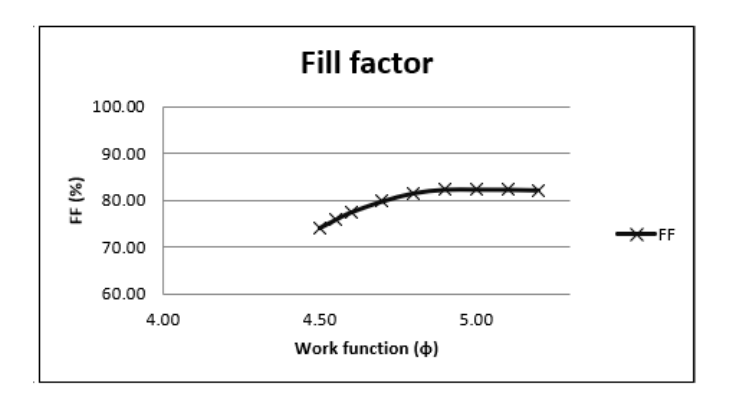


Figure 8: Fill Factor (FF) at various MoW metal work function

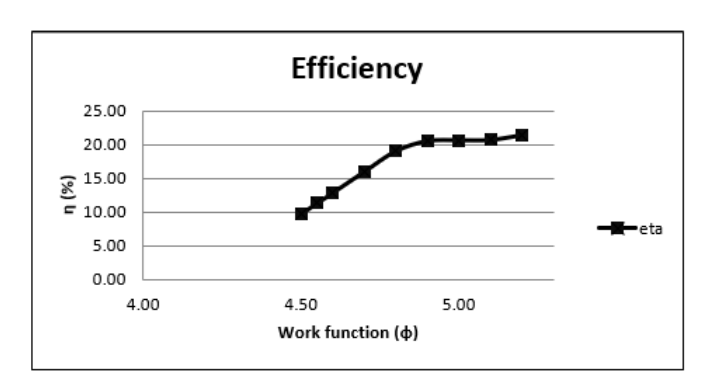


Figure 9: Efficiency at various MoW metal work function

Figure 6 to Figure 9 show the simulation results at various metal back contact work function values. From these results, it can be seen that the overall performance of  $V_{OC}$ ,  $J_{SC}$ , Fill Factor (FF) and Efficiency, respectively, are increased with the increments of the back contact work function values from 4.50eV to 5.2eV.

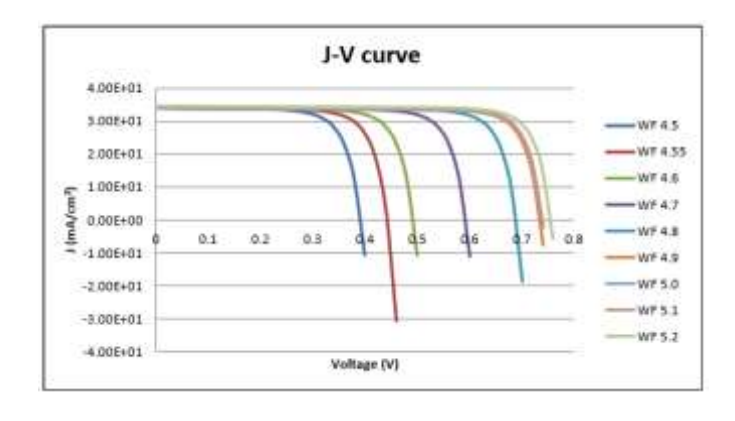


Figure 10: J-V curve at various MoW metal work function



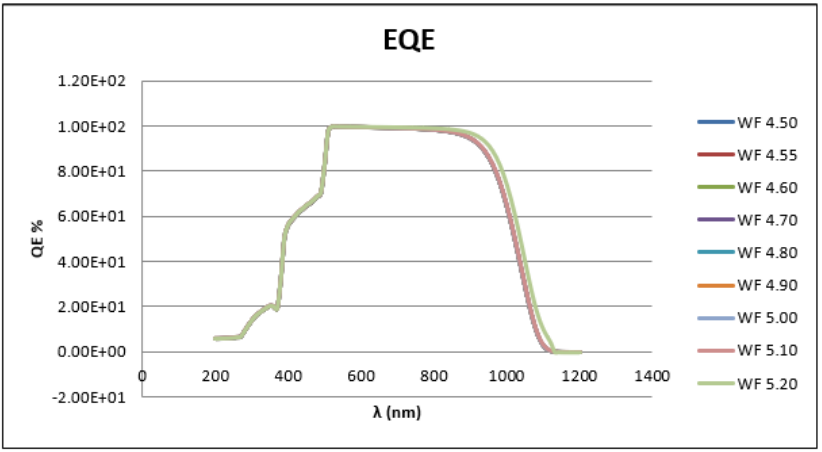


Figure 11: EQE curve at various MoW metal work function

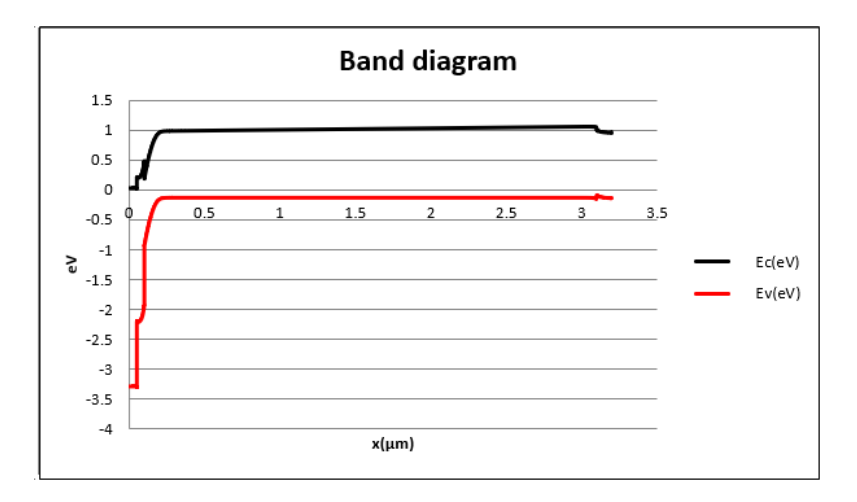


Figure 12: Band diagram of CIGS solar cell (flatband).

To complete the results, Figure 10 to Figure 12 shows the J-V curve, EQE and the simulated CIGS solar cell band diagram. These figures also show improvements when the back contact work function values are increased.

If the band diagram at the CIGS absorber layer and MoSe<sub>2</sub> layer interface (M-S junction energy band) is zoomed in, it can be observed that the Ec and Ev curve will change when the work function is increased from flatband to 5.2 eV as shown in Figure 13 below.

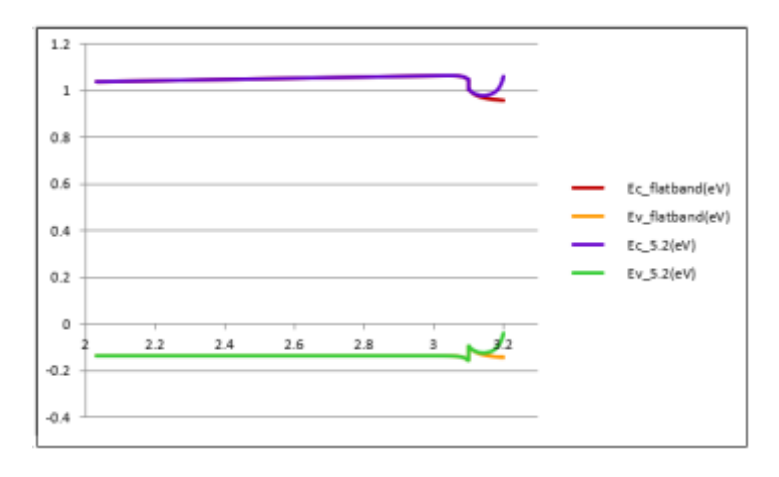


Figure 13: Comparison between Ec, Ev(flatband) and Ec, Ev (at work function 5.2eV) at the CIGS absorber layer and MoSe<sub>2</sub> layer interface (M-S junction).

When the work function is increased to 5.2eV, we notice that the Ec and Ev curves are bending upwards. The high work function back contact reduces the potential barrier at the back interface, and introduces an electric



field to suppress the recombination of photogenerated electrons and holes [Gunawan et. al] and [5]. This explains the efficiency improvement when the energy bands at the back interface bend upwards.

To achieve a higher work function back contact, the study continues with simulations by using Density Functional Theory (DFT). The calculations were conducted using Winmostar Quantum Espresso software on as detailed below.

# Simulations using Winmostar Quantum Espresso software

The first step is calculating and comparing the work functions for various metals as tabulated in Table 3. The results were compared to [6] as shown in Table 4.

Table 3: Simulation results of various metal work function using Winmostar Quantum Espresso software (with vacuum level fixed at 25 Angstrom)

	ecutt	k-point	Work function
Ag	50	12x12x12	4.59
Al	25	12x12x12	4.20
Mo	50	12x12x12	4.56
Au	45	9x9x9	5.45
W	60	8x8x8	4.75

Table 4: Comparison between the calculated work function for various metals and [6].

	Work function (simulation)	Work function ([6])
Ag	4.59	4.26 – 4.74
Al	4.20	4.06 – 4.26
Мо	4.56	4.36 – 4.95
Au	5.45	5.10 – 5.47
W	4.75	4.32 – 5.22

Table 3 and Table 4 show the DFT calculations for various metals. By comparing with [6], the DFT calculations are considerably acceptable because all the calculation values are within the range of those in [6].

After that, DFT calculations were conducted for various Mo plane in order to get the highest work function.

Table 5: Comparison of Work Function (eV) for Mo between simulation and [6] and [10] at various plane.

Plane	(111)	(110)	(100)	(310)
Mo (simulation)	3.96	4.57	3.84	3.88
[6]	4.55	4.95	4.53	-
[10]	3.76	4.53	3.76	3.53

Table 5 shows that the Mo work function value is the highest at plane (110). This finding agrees with [6] and [10] respectively.

# ISSN No. 2454-6186 | DOI: 10.47772/IJRISS | Volume IX Issue X October 2025

Table 6: Comparison of Work Function (eV) for Mo and W at plane (110) between simulations and [6] and [10].

	Simulation	[6]	[10]
Mo	4.57	4.95	4.53
W	4.79	5.22	4.80

The study then continued by performing DFT calculations for Mo and Tungsten (W) at plane (110), and the results were again compared with [6] and [10] as shown in Table 6. The DFT calculations are acceptable as compared to [6] and [10] because the DFT calculations only results in approximation values.

This study chooses to alloy Mo with W for a fact that both Mo and W characteristics are inherent such as corrosion resistance and excellent conductivity. Both Mo and W reflectivity curves are also nearly alike [7].

The next step is a DFT calculations for Mo alloyed with W at various molecular percentage and the results are tabulated in Table 7 and shown in Figure 14 respectively.

Table 7: Simulation of Work Function (eV) for Mo alloyed with W at various molecular percentage.

Material	Work Function (eV)
Мо	4.57
Mo <sub>0.875</sub> W <sub>0.125</sub>	4.77
Mo0.75W <sub>0.25</sub>	4.76
Mo0.625W <sub>0.375</sub>	4.78
Mo <sub>0.5</sub> W <sub>0.5</sub>	4.72
Mo <sub>0.375</sub> W <sub>0.625</sub>	4.75
Mo <sub>0.25</sub> W <sub>0.75</sub>	4.75
Mo <sub>0.125</sub> W <sub>0.875</sub>	4.78
W	4.79

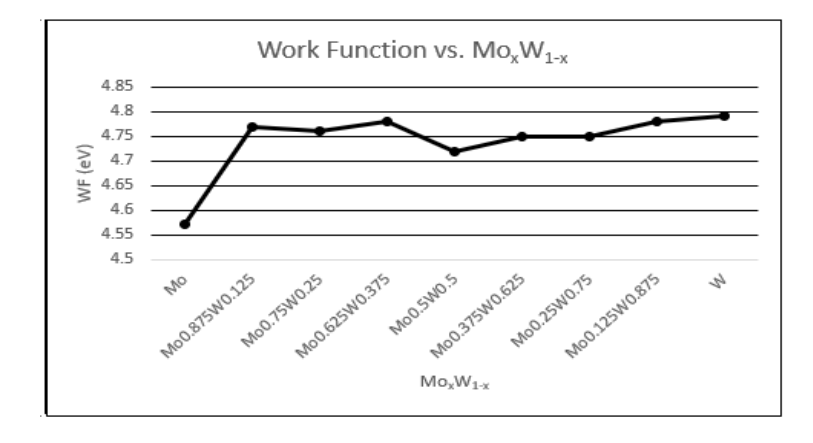


Figure 14: Simulation of Work Function (eV) vs MoxW1-x.

The results clearly show a significant increase in the surface work function when Mo is alloyed with W. The surface work function increases from 4.57eV to 4.78eV after a smaller percentage of W is alloyed on the Mo surface. These results show a promising finding to help improve the CIGS solar cell efficiency (by increasing the metal back contact work function value).





# CONCLUSION AND FUTURE WORK

In conclusion, this study provides valuable insights into the factors influencing the CIGS solar cell efficiency. From the simulations both using SCAPS-1D and DFT calculations, the work function of the metal back contact effects the cell performance.

Based on SCAPS-1D simulation, the CIGS solar cell efficiency increased significantly from 9.82% to 20.69% with the increase of metal back contact value, from 4.50eV to 5.10eV, respectively due to enhancement of  $V_{OC}$ ,  $J_{SC}$ , and Fill Factor (FF). The desired work function value of the back contact is above 4.90eV.

In the meantime, based on DFT calculations, plane orientation (110) exhibits the highest work function value for Mo. By alloying Mo with W, the surface work function of the back contact can be increased from 4.57eV to 4.79eV at plane orientation (110). Substitutional alloy (surface alloy) of Mo<sub>0.875</sub>W0<sub>.125</sub> to Mo<sub>0.625</sub>W<sub>0.375</sub> are sufficient to increase the work function value of the back contact significantly. Alloying Mo with a small percentage of W helps to increase the back contact work function while retaining the other properties of Mo back contact.

Future research should aim to experimentally materialize alloying Mo with W. One of the key challenges for this would be to choose a suitable and feasible depositing method of W on the surface of Mo because W possess a very high melting point.

Other than that, there is also a need to examine the effects of MoW alloy metal as the back contact. The current Mo back contact will produce MoSe<sub>2</sub> layers in between the CIGS absorber layer and Mo back contact. Thus, an investigation on the effects of introducing W metal element on top of Mo should be conducted, and how it will affect the MoSe<sub>2</sub> layer.

This study focuses on the effect of metal back contact work function to the overall CIGS solar cell efficiency. In the future, this study can be further expanded to include investigations on ways to improve the front contact, buffer layer and absorber layer as well for a holistic approach to efficiency CIGS solar cell improvements. And to further enhance the findings, investigations should also be conducted on cost effectiveness, scalability, and environmental impacts.

# ACKNOWLEDGEMENTS

The authors would like to thank University Technical Malaysia Melaka (UTeM) and the Centre for Research and Innovation Management (CRIM), UTeM for their research support.

# REFERENCES

- 1. R.K. Pachauri, L.A. Meyer (eds.), IPCC, 2014: Climate change 2014: Synthesis Report. Contribution of Working Groups I, II and III to the Fifth Assessment Report of the Intergovernmental Panel on Climate Change. IPCC, Geneva, Switzerland, 151 pp.
- 2. H. Ritchie et. Al, 2020. CO<sub>2</sub> and Greenhouse Gas Emissions. Published online at OurWorldInData.org
- 3. The National Renewable Energy Laboratory, NREL. US Department of Energy, Office of Energy Efficiency and Renewable Energy.
- 4. Takuya Kato et. Al, Record Efficiency for thin-film polycrystalline solar cells up to 22.9% achieved by Cs- Treated Cu(In,Ga)(Se,S)<sub>2</sub>
- 5. Dongxiao Wang et.al , Tuning the Work Function of the Metal Back Contact toward Efficient Cu<sub>2</sub>ZnSnSe<sub>4</sub> Solar cells, Solar RRL 2021, 5, 2000391, Nov 16, 2020
- 6. David R. Lide, CRC Handbook of Chemistry and Physics, 84th Edition, CRC Press
- 7. W. W. Coblentz, The Reflecting Power of Various Metals
- 8. Sanghyun Lee et al., Engineering of Effective back-contact barrier of CZTSe: Nanoscale Ge solar cells MoSe<sub>2</sub> defects implication, Solar Energy 194 (2019)114-120
- 9. Winmostar Quantum Espresso, X-Ability Co. Ltd
- 10. [Materialsproject.org





- 11. M. F. Rahman et al., A qualitative Design and optimization of CIGS-based Solar Cells with Sn2S3 Back Surface Field: A plan for achieving 21.83% efficiency, Multidisciplinary, 2023.
- 12. H. K. Park and W. Jo, Flexible Cu(In,Ga)Se2 photovoltaics for bending applications, Journal of Materials Chemistry C, Royal Society of Chemistry, 2025.
- 13. S. Ramesh, Energy yield framework to simulate thin film CIGS solar technology performance, Scientific Reports, Nature Publishing Group, 2025.
- 14. M. Fathi et al., Study of Thin Film Solar Cells in High Temperature Condition, Procedia Engineering, 2015.
- 15. C. L. Chuang, M. W. Chang, N. P. Chen, C. C. Pan, and C. P. Liu, Improving Performance of CIGS Solar Cells by Annealing ITO Thin Films Electrodes, Advances in Materials Science and Engineering, Hindawi Publishing Corporation, 2015.
- 16. M. E. M. Soudagar, Effect of electron transport layer thickness and solar cell performance in CIGS devices, Solar Energy, Elsevier, 2025.
- 17. A. Elmelouky, In-depth study of CIGS layer properties with silicon layer impact for solar cell enhancement, Solar Energy Materials & Solar Cells, Elsevier, 2025.
- 18. N. Khoshsirat et al., Numerical simulation of CIGS thin film solar cells using SCAPS-1D, Pertanika Journal of Science & Technology, 2015.
- 19. M. Izaki et al., Finding a way to boost efficiency of CIGS solar cells, Progress in Photovoltaics, Wiley, 2015.
- 20. Jackson P., Hariskos D., Lotter E., Paetel S., Wuerz R., Menner R., Wischmann W., Powalla M., New world record efficiency for Cu(In,Ga)Se2 thin-film solar cells beyond 20%, Prog. Photovoltaics: Res. Appl., Volume 19, 2011